



Adsorption-coupled reduction of bromate by Fe(II)–Al(III) layered double hydroxide in fixed-bed column: Experimental and breakthrough curves analysis



Qi Yang^{a,b,*}, Yu Zhong^{a,b}, Xiaoming Li^{a,b,*}, Xin Li^{a,b}, Kun Luo^c, Xiuqiong Wu^{a,b}, Hongbo Chen^{a,b}, Yang Liu^{a,b}, Guangming Zeng^{a,b}

^a College of Environmental Science and Engineering, Hunan University, Changsha 410082, China

^b Key Laboratory of Environmental Biology and Pollution Control, Hunan University, Ministry of Education, Changsha 410082, China

^c Department of Bioengineering and Environmental Science, Changsha College, Changsha 410003, China

ARTICLE INFO

Article history:

Received 25 June 2014

Received in revised form 19 January 2015

Accepted 27 January 2015

Available online 3 February 2015

Keywords:

Fe(II)–Al(III) layered double hydroxide

Bromate

Fixed-bed column

Adsorption-coupled reduction

Breakthrough curve

ABSTRACT

In this study, the bromate removal was investigated in continuous fixed-bed column using Fe(II)–Al(III) layered double hydroxide (LDH). With increase of column bed depth from 1.0 to 3.0 cm, breakpoint time (t_b) increased from 51 to 175 h while throughput volume raised from 12.24 to 42.00 L at breakthrough point. The bromate removal was attributed to the reduction of Fe(II) present in LDH. The breakthrough curve was simulated well by Thomas model, but BDST model was the only effective to initial part (1–10%). The maximum removal capacity (N_0) calculated by Thomas model reached 71.01 $\mu\text{mol/g}$ at flow rate (3 mL/min).

© 2015 The Korean Society of Industrial and Engineering Chemistry. Published by Elsevier B.V. All rights reserved.

Introduction

Bromate (BrO_3^-), a major disinfection by-product (DBP) when bromide-containing water is treated by ozonation or other advanced oxidation, has raised great concerns because of its carcinogenic potency in humans [1]. For children, ingestion of 60–120 mL of 2% bromate would have serious poisonings [2]. Deshimaru et al. [3] reported a range of ages with acute renal failure due to bromate poisoning. In view of the above poisonous effects of bromate on human health, the World Health Organization (WHO) and United States Environmental Protection Agency (USEPA) have set a maximum contaminant level (MCL) for bromate in drinking water of 10 $\mu\text{g/L}$ (0.078 $\mu\text{mol/L}$) [4]. Pilot-scale and full-scale drinking water studies have shown the bromate in the range of 0–60 $\mu\text{g/L}$ was formed under various water conditions [5]. Therefore, the effective methods for bromate removal need to be investigated.

Studies have been performed for the bromate removal by different materials such as activated carbon [6], zero-valent iron

[7], metal oxide [8], and membrane materials [9]. Recently, layered double hydroxides (LDHs), also named anionic clays with high anion exchange capacity and large surface area, have increasingly received attention to bromate uptake from aqueous solutions. Chitrakar et al. [10] evaluated the effect of calcined Mg–Al LDH on bromate removal, and indicated that uncalcined LDH exhibited no bromate uptake, and calcined LDH reduced the bromate concentration in aqueous solutions below the accepted level of 0.078 $\mu\text{mol/L}$. Moreover, LDH could exhibit highly adsorption properties for the pollutants by the intercalation of molecules, such as 2,4-dihydroxybenzophenone-5-sulfonate (DHBS) and other molecules [11,12]. However, within the LDHs family, Fe(II)–Al(III) LDH showed the special adsorption-coupled reduction capability for bromate due to the existence of Fe(II) [13,14]. In our previous study, Fe–Al LDH (SO_4 type) was synthesized by using ultrasound-assisted co-precipitation method and the batch experimental results indicated that bromate could be rapidly reduced to bromide [15].

Batch reactor can be operated easily in the laboratory study, but batch mode is not appropriate for industrial applications because of a need for continuous flow of wastewater and the large volume involved. In the ion exchange, adsorption and reduction process, the fixed-bed column has been proven to be an effective process for

* Corresponding authors at: College of Environmental Science and Engineering, Hunan University, Changsha 410082, China. Tel.: +86 731 88822829; fax: +86 731 88822829.

E-mail addresses: yangqi@hnu.edu.cn (Q. Yang), xmli@hnu.edu.cn (X. Li).

Nomenclature

t_b	breakpoint time (h) (when $C_t/C_0 = 1\%$ was present in the column effluent)
t_e	exhaust time (h) (when $C_t/C_0 = 97\%$ was present in the column effluent)
V_b	throughput volume at breakthrough (L)
V_t	throughput volume at any instant of time t (L)
v	the linear velocity (cm/h)
Z	the bed depth of column (cm)
w	the mass of the Fe–Al LDH (g)
k_{BA}	the kinetic constant of BDST model ($L/\mu\text{mol h}$)
k_{Th}	the rate constant of Thomas model ($L/\mu\text{mol h}$)
N_0	the maximum bromate removal capacity ($\mu\text{mol/g}$)
C_0	initial bromate concentration ($\mu\text{mol/L}$)
C_t	outlet bromate concentration ($\mu\text{mol/L}$)
$\varepsilon\%$	the average percentage error
R^2	regression coefficient

continuous flow system, due to the simplicity, ease of operation and handling [16,17]. The performance of fixed-bed column was described through the concept of breakthrough curve in many studies [18–20]. The time of breakthrough and the shape of the breakthrough curve are very important characteristics for determining the operation and the dynamic response of fixed-bed column [21]. Various mathematical models, such as the bed depth service time (BDST) model, Yoon–Nelson model, Clark model and Thomas model were used to evaluate and predict the removal performance of inexpensive adsorbents for heavy metals removal in fixed-bed column [22,23].

Most of the reported studies about bromate removal by LDHs are conducted in batch mode [10,14]. However, no study has been reported in column mode. As a continuation of our previous batch experiments [15], the aim of the present work is to explore the possibility of utilizing Fe–Al LDH for the adsorption-coupled reduction of bromate from solutions in fixed-bed column. In addition, the effects of various parameters such as bed depth, flow rate, and initial bromate concentration on the shape of the breakthrough curve were examined, respectively. The dynamic process was modeled by BDST model and Thomas model. Error analysis was carried out to test the adequacy and accuracy of the models.

Experimental

Synthesis and characterization of Fe–Al LDH

In this research, the Fe–Al LDH was synthesized by using an ultrasound-assisted co-precipitation method according to our previous publication [15]. The structure of Fe–Al LDH was characterized using an IRAffinity-1 spectrometer (Shimadzu FTIR-8400S, Japan) with KBr disk method at a resolution of 4 cm^{-1} , and 10 scans were recorded in a range of $400\text{--}4000\text{ cm}^{-1}$ to ensure good signal to noise ratio.

Column experiments

The fixed-bed column was made of Pyrex glass tube with 30 cm long and 2.5 cm internal diameter (Fig. 1). To avoid any spaces in the bed, the column was packed with non-uniform size (effective diameter $74\text{--}149\ \mu\text{m}$) Fe–Al LDH. Quartz sand (10 cm depth) was placed at the bottom of the bed to support LDH particles. The bed

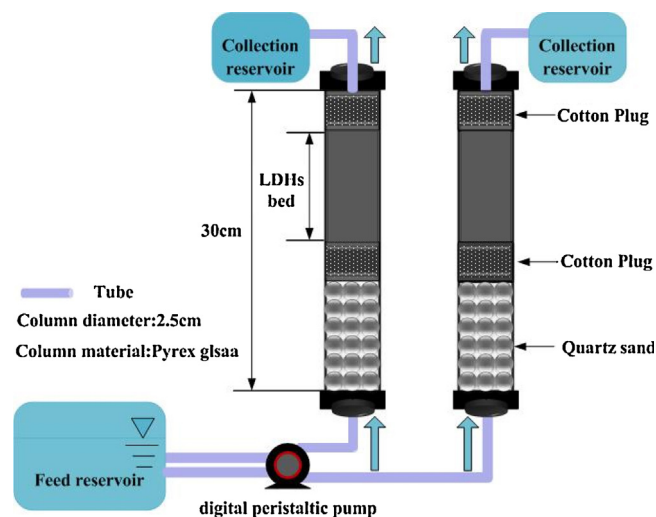


Fig. 1. Schematic diagram of Fe–Al LDH fixed-bed column system.

depth of 1, 2 and 3 cm in column contained 4.99, 9.98 and 14.97 g of LDH, respectively. The column was operated continuously at room temperature ($25 \pm 1^\circ\text{C}$) in up-flow mode using digital peristaltic pump (DHL-A, Shanghai) at a constant linear flow rate of 3, 4 and 6 mL/min. Synthetic bromate solution was prepared in distilled water using anhydrous NaBrO_3 with initial bromate concentrations of 3.125 and $6.250\ \mu\text{mol/L}$. The pH of the influent was adjusted at a constant value of 7.0 ± 0.1 .

Analytical methods

Bromate and bromide were measured by a single-column ion chromatograph (Dionex ICS-900, USA) with a low-conductivity mobile phase. 9.4 mM sodium carbonate (Na_2CO_3) and 1.8 mM sodium bicarbonate (NaHCO_3) were used as the eluent at a flow rate of 1.0 mL/min. The separation column (Dionex IonPac AS19, 4.0 mm ID \times 250 mm) was operated at 40°C . The concentration of iron in effluent was analyzed by atomic absorption spectrometry (PEAA-700, USA).

Breakthrough curves

Column “breakthrough” is defined as phenomenon when the effluent concentration from the column is about 3–5% of the influent concentration [24]. However, breakthrough at 1% is also considered on basis of effluent discharge limit [25]. In this study, the breakpoint time t_b (h) was chosen as the time when the concentration of the effluent is 1% ($0.078\ \mu\text{mol/L}$), namely the maximum contaminant level for bromate discharge. Exhaustion was usually considered when the effluent concentration was close to influent concentration for long period. The exhaustion time t_e (h) was considered when effluent bromate reached 97% of influent concentration.

Two major parameters, the contact time (or the empty bed residence time, EBRT) and the LDH exhaustion rate (LER), were chosen to evaluate the performance of fixed-bed column. LER is defined as the mass of Fe–Al LDH exhausted per volume of liquid treated at breakthrough point:

$$\text{LER} = \frac{\text{mass of LDH}}{\text{volume treated at breakthrough point}} \quad (1)$$

EBRT is the time required for the liquid to fill the empty column [26], which is defined as:

$$\text{EBRT (min)} = \frac{\text{bed volume}}{\text{volumetric flow rate}} \quad (2)$$

Larger EBRT ensures more time for the bromate removal by Fe–Al LDH. Meanwhile, lower LER indicates good performance of the fixed-bed column.

Error analysis

In order to verify the most applicable model to describe the performance of breakthrough curves, error analysis was performed. Generally, linear regression coefficient (R^2) shows the fit between experimental data and linearized forms of models while the average percentage error ($\epsilon\%$) is used to illustrate the fit between experimental and theoretical values of C_t/C_0 used for plotting breakthrough curves. The $\epsilon\%$ is calculated according to the following equation [27]:

$$\epsilon\% = \frac{\sum_{i=1}^N [(C_t/C_0)_{\text{exp}} - (C_t/C_0)_{\text{theo}}] / (C_t/C_0)_{\text{exp}}}{N} \times 100 \quad (3)$$

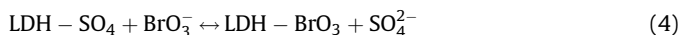
where N is the number of measurements.

Results and discussion

Column experiment and proposed mechanism of bromate removal

In order to study the behavior of the adsorption-coupled reduction taken place in the column, the time-dependent concentrations of bromate (BrO_3^-), bromide (Br^-) and total Br were measured under the stable operating conditions as initial bromate concentration $6.25 \mu\text{mol/L}$, bed depth 1 cm and flow rate 4 mL/min (Fig. 2).

From Fig. 2a, it was clear that Fe–Al LDH showed perfect adsorption-coupled reduction ability because the exhaust time is nearly 275 h at the operating conditions. The adsorption of bromate on Fe–Al LDH in the initial stage was mainly via anion exchange mechanism which could be described by the following equation:



Meanwhile, the sulfate in the effluent also demonstrated the mechanism (Fig. 2b). Similar phenomenon was reported by Chitrakar and co-workers that the uptake of nitrate, bromate, or sulfate on the novel LDH of Mg and Al ($\text{MgAl}_4\text{-Cl}$) was accompanied by a release of chloride into the solution [28].

After approximate 40 h of operation, bromate appeared in the effluent and the bromide concentration began to drop. This fact demonstrated that the Fe–Al LDH could not contribute to the adsorption-coupled reduction of bromate when it started to become saturated. On the other hand, the adsorption-coupled reduction process was very significant since the bromate concentration in effluent was still under the MCL even after 51 h. As experiment proceeded, bromate concentration in the outlet was the same as that in the inlet one after 275 h (Fig. 2a), which indicated that the adsorption-coupled reduction capacity of Fe–Al LDH had been exhausted. Monitoring of the effluent pH during the column operation showed the value of pH increased from 7.06 to 7.55 at initial 60 h (Fig. 2b), since the hydroxyl ions were produced during bromate reduction by Fe^{2+} at neutral condition (Eq. (5)).



As the bromate removal performance of the column decreased, the effluent pH declined to 6.26, which should be attributed to the formation of ferric sulfate in effluent. In addition, the total iron in the effluent led by the release of Fe^{3+} from LDH decreased with the operation time increased, which also illustrated that the bromate reduction gradually terminated with the exhaustion of Fe(II) in Fe–Al LDH.

The Fourier transform infrared (FT-IR) spectra of the Fe–Al LDH functional group before and after saturation with bromate were

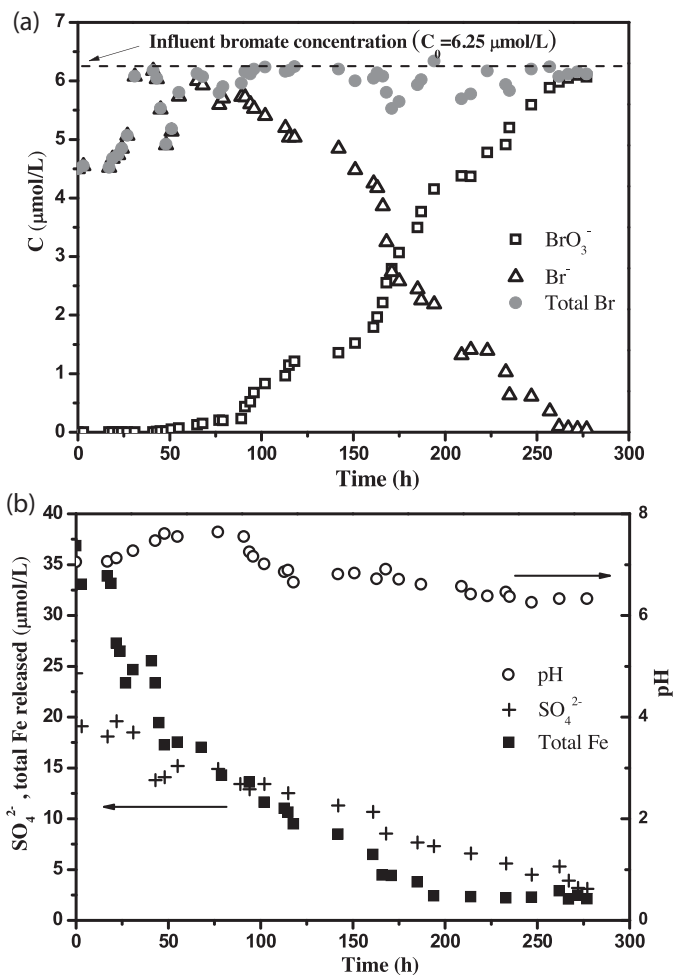


Fig. 2. (a) Time variation of bromate, bromide and total Br concentrations. (b) Release of sulfate and total Fe into solution. The solution pH was not controlled during the experiment (initial pH 7.06, initial bromate concentration $6.25 \mu\text{mol/L}$, bed depth 1 cm and flow rate 4 mL/min).

presented in Fig. 3. The particularly broad band of fresh Fe–Al LDH was observed between 3400 and 3500 cm^{-1} , which corresponded to the stretching vibration of the hydroxyl groups of LDH layers [29,30]. The weak absorption peak at 2358 cm^{-1} was possibly attributed to hydrogen bonded or ionized compound structure.

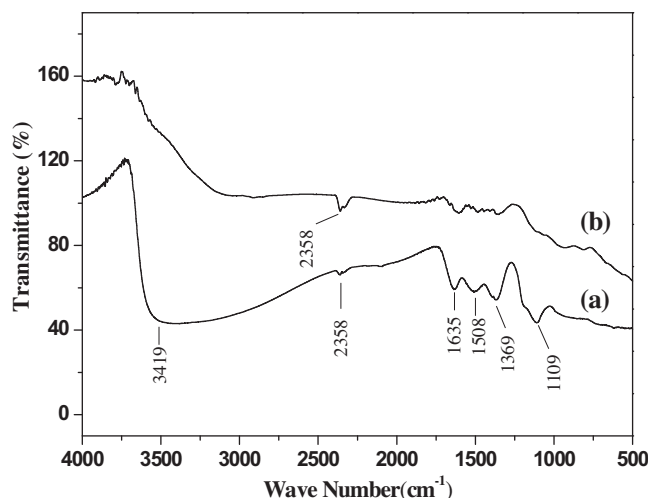


Fig. 3. FT-IR spectra of (a) fresh Fe–Al LDH and (b) exhausted Fe–Al LDH.

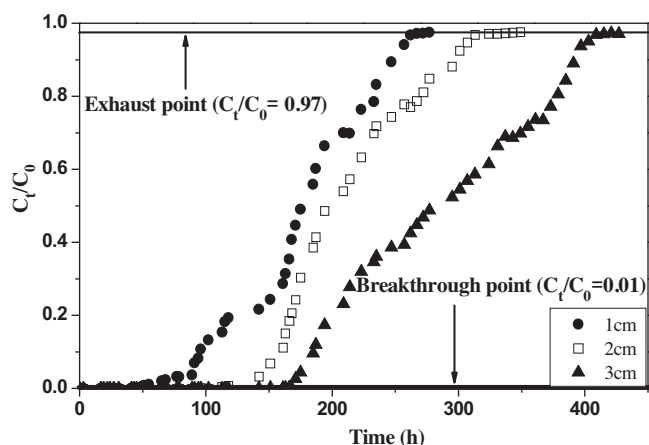


Fig. 4. Breakthrough curves for bromate removal at different bed depth (initial bromate concentration $6.25 \mu\text{mol/L}$ and flow rate 4 mL/min).

The obvious peak at 1635 cm^{-1} could be assigned to the water bending vibration of interlayer water [31]. Even though greatest care was taken to exclude carbonate from the system, carbonate was sometimes found in the interlayer space, resulting in the peak at 1369 cm^{-1} , while the peaks at around 1508 cm^{-1} indicated the presence of HCO_3^- in the interlayer space [32]. The strongest peak at 1109 cm^{-1} was due to the SO_4^{2-} intercalated in the interlayer space [31]. After saturation with bromate, the FT-IR spectra of Fe–Al LDH changed obviously. As explained in our previous study, the adsorbed bromate reacted with Fe^{2+} in LDH and the LDH translated into a mixture of poorly crystalline goethite, amorphous aluminum hydroxide, and LDH residue [15]. So the band observed at 3419 cm^{-1} became weak with the adsorption of bromate and bromide on LDH, the absorption peak at 2358 cm^{-1} was strengthened. The band from 1109 to 1635 cm^{-1} became weaker, demonstrating that SO_4^{2-} and CO_3^{2-} in the interlayer space already had released in aqueous solutions.

Effects of operating parameters on column performance

Effect of bed depth

Fig. 4 shows the breakthrough curve dynamics obtained from columns with the bed depth 1, 2 and 3 cm. In this section, other parameters such as initial bromate concentration and flow rate were fixed at $6.25 \mu\text{mol/L}$ and 4 mL/min , respectively. The increase in bromate removal with that in bed depth was attributed to the increase of Fe–Al LDH doses in higher bed which provided more active sites and more electrons to bromate removal.

From Table 1, it can be seen that the breakpoint time (t_b) were 51, 142 and 175 h at 1, 2 and 3 cm bed depth, respectively, suggesting that the breakthrough time increased with bed depth. Meanwhile, the throughput volume at breakthrough (V_b) of the bed

Table 1
Parameters in fixed-bed column for bromate removal by Fe–Al LDH.

Initial bromate concentration ($\mu\text{mol/L}$)	Flow rate (mL/min)	Bed depth Z (cm)	t_b (h)	V_b (L)	EBRT (min)	LER (g/L)
6.250	4	1	51	12.24	1.23	0.41
6.250	4	2	142	34.08	2.45	0.29
6.250	4	3	175	42.00	3.69	0.36
3.125	3	1	267	48.06	1.64	0.10
3.125	4	1	187	44.88	1.23	0.11
3.125	6	1	115	41.40	0.82	0.12

depth of 1, 2 and 3 cm were calculated and the values were 12.24, 34.08 and 42.00 L, respectively. The results indicated that the increase of bed depth is favorable to improve the bed performance in removing bromate. The good performance can be the result of the more contact opportunities between the bromate and Fe–Al LDH. The phenomena in this study were similar to the reduction of nitrate by nano-Fe/Cu particles in packed column [17].

Effect of flow rate

The effect of flow rate on the bromate removal in fixed-bed column with a bed depth of 1 cm was investigated. The flow rate was changed in the range of 3, 4 and 6 mL/min while maintaining the initial bromate concentration constantly at $3.125 \mu\text{mol/L}$. The breakthrough curves of bromate are illustrated in Fig. 5. It was noticed that more processing time was required to reach the breakthrough for low flow rate. The t_b were found to be 267, 187 and 115 h for flow rate at 3, 4 and 6 mL/min , respectively, with corresponding empty bed contact time (EBRT) of 1.64, 1.23 and 0.82 min. The results demonstrated that an increase in flow rate caused the decrease of the t_b due to a decrease in EBRT. But the lower of EBRT, the less effective of the diffusion process, thus resulting in lower removal efficiency [19]. With increasing flow rate, the breakthrough curves became steeper and V_b decreased from 48.06 to 41.40 L. This behavior is similar to report by Ghorai et al. [33] and can be explained in the following way: if the flow rate is too fast, the solute in the column have not enough residence time to reach adsorption equilibrium, it will leave the column before equilibrium occurs. So lower flow rate would be beneficial for bromate removal in Fe–Al LDH column.

Effect of initial bromate concentration

Experiments were carried out to evaluate the efficiencies of bromate removal by Fe–Al LDH in different initial bromate concentration (3.125 and $6.250 \mu\text{mol/L}$). In these series of experiments, the flow rate and bed depth was fixed as 4 mL/min and 1 cm, respectively. As shown in Table 1, the LER was 0.11 and 0.41 g/L at initial bromate concentration of 3.125 and $6.250 \mu\text{mol/L}$, respectively. The lower LER suggested good performance of the fixed-bed column and indirectly indicated the Fe–Al LDH was an excellent material for bromate removal. With the initial bromate concentration increasing from 3.125 to $6.250 \mu\text{mol/L}$, the value of t_b decreased from 187 to 51 h and subsequently, the V_b decreased from 44.88 to 12.24 L. This implied that the increase of initial concentration accelerated the consumption of Fe–Al LDH.

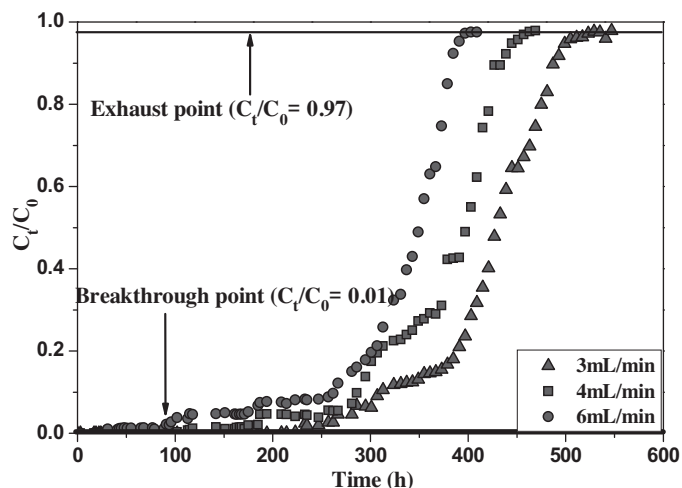


Fig. 5. Breakthrough curves for bromate removal at different flow rate (initial bromate concentration $6.25 \mu\text{mol/L}$ and bed depth 1 cm).

Modeling of bromate removal in the column

In order to describe the fixed-bed column behavior, two classic kinetic models, bed depth service time (BDST) and Thomas models were used to fit the experimental data in the column.

Application of the BDST model

The BDST model based on Bohart–Adams equation is one of the most applied models in column studies [34]. The Bohart–Adams equation model can be represented as:

$$\ln\left(\frac{C_0}{C_t} - 1\right) = \ln(e^{k_{BA}N_bZ/v} - 1) - k_{BA}C_0t \quad (6)$$

But to follow the Bohart–Adams approach at least nine individual column tests must be conducted to collect the required laboratory data [35]. Therefore, Hutchin [36] simplified the Bohart–Adams equation and presented a linear relationship between the bed depth and service time, called BDST model [Eq. (7)], which requires only three fixed-bed tests to collect the necessary data.

$$t_b = \frac{N_bZ}{C_0v} - \frac{1}{k_{BA}C_0} \ln\left(\frac{C_0}{C_t} - 1\right) \quad (7)$$

where t_b is the service time at breakthrough point (h), C_0 and C_t are initial and breakthrough solute concentration ($\mu\text{mol/L}$), respectively. N_b is dynamic removal capacity of the fixed-bed column ($\mu\text{mol/cm}^3$), k_{BA} ($\text{L}/\mu\text{mol h}$) is the kinetic constant, and v (cm/h) is the linear velocity calculated by dividing the flow rate (Q) by the column section area. Eq. (7) can be rewritten as in the form of a straight line:

$$t_b = aZ + b \quad (8)$$

where

$$a = \text{slope} = \frac{N_b}{C_0v} \quad (9)$$

$$b = \text{intercept} = -\frac{1}{k_{BA}C_0} \ln\left(\frac{C_0}{C_t} - 1\right) \quad (10)$$

Thus, a linear plot of bed depth (Z) against time (t_b) was employed to determine the parameters of dynamic removal capacity (N_b) and kinetic constant (k_{BA}) from the intercepts and slopes.

The results of bed depth (Z) and service time at breakthrough point (t_b) are plotted in Fig. 6 according to Eq. (8) for 1%, 50% and 90% breakthrough at column bed depth of 1, 2 and 3 cm. The slope, intercept, R^2 and $\varepsilon\%$ at other breakthrough values were calculated in a similar way plotting service time with bed depth, and results are listed in Table 2.

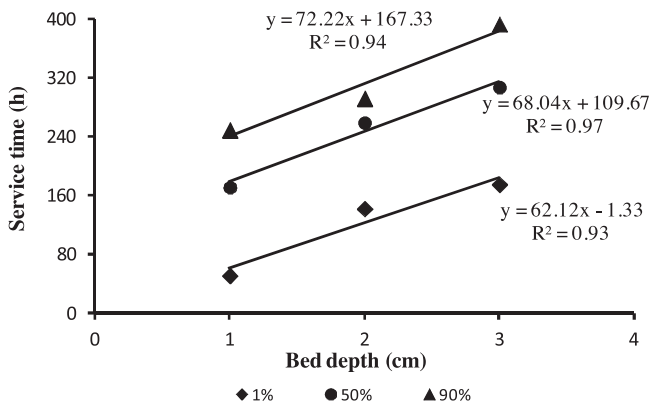


Fig. 6. BDST model for bromate removal at various breakthrough.

Table 2

Kinetics model parameters and comparison between the two kinetic models.

Breakthrough (%)	Slopes a	Intercepts b	BDST model			
			k_{BA} ($\text{L}/\mu\text{mol h}$)	N_b ($\mu\text{mol/L}$)	R^2	$\varepsilon\%$
1 ^a	62.12	-1.33	0.55×10^{-3}	18.99×10^3	0.93	6.67
10	67.01	-0.67	0.52×10^{-3}	20.49×10^3	0.91	9.91
30	67.91	41.34	0.33×10^{-3}	20.76×10^3	0.91	17.24
50 ^a	68.04	109.67	0	20.81×10^3	0.97	16.31
70	70.11	124.31	0.11×10^{-3}	21.44×10^3	0.91	28.94
90 ^a	72.22	167.33	0.21×10^{-3}	22.09×10^3	0.94	28.91

C_0 ($\mu\text{mol/L}$)	Q (mL/min)	Z (cm)	Thomas model			
			k_{Th} ($\text{L}/\mu\text{mol h}$)	N_0 ($\mu\text{mol/g}$)	R^2	$\varepsilon\%$
6.250	4	1	4.96×10^{-3}	30.98	0.91	5.22
6.250	4	2	8.02×10^{-3}	33.83	0.86	6.61
6.250	4	3	6.83×10^{-3}	50.03	0.81	7.97
3.125	3	1	6.30×10^{-3}	71.01	0.90	8.11
3.125	4	1	7.49×10^{-3}	53.18	0.86	11.62
3.125	6	1	9.15×10^{-3}	46.98	0.76	10.49

^a BDST plots for these different breakthrough percentages at bed depth of 1, 2 and 3 cm were plotted and is shown in Fig. 6.

As seen from Table 2, the values of R^2 are all above 0.91 but the $\varepsilon\%$ was more than 16.31% after breakthrough value was 30%. The error analysis suggested that BDST model could not be validated for all breakthrough percentage and could only be used to simulate the initial part of the breakthrough curve. As the breakthrough percentage increased from 1 to 90%, it was also a consistent rise in slopes from 62.12 to 72.22 and in dynamic removal capacity from 18.99×10^3 to $22.09 \times 10^3 \mu\text{mol/L}$. At lower breakthrough value, some active sites of the Fe–Al LDH still unoccupied by bromate and thus the column remained unsaturated. Therefore the dynamic removal capacity in such low breakthrough condition was bound to be lower than the full bed capacity of the Fe–Al LDH.

Application of the Thomas model

The Thomas model is another most general and widely used method in column performance theory. This approach focused on the estimation of characteristics parameters such as maximum removal capacity (N_0) and the reaction rate constant (k_{Th}). The model has the following form:

$$\frac{C_0}{C_t} = 1 + \exp\left(\frac{k_{Th}}{Q}(N_0w - C_0V_{eff})\right) \quad (11)$$

where k_{Th} ($\text{L}/\mu\text{mol h}$) is the Thomas rate constant, N_0 ($\mu\text{mol/g}$) is maximum removal capacity, C_0 and C_t ($\mu\text{mol/L}$) are the inlet and outlet concentration, respectively. w (g) is the mass of the Fe–Al LDH, and t (h) stands for the flow time. A linear plot of $\ln[(C_0/C_t) - 1]$ against time (t) was employed to determine values of k_{Th} and N_0 from the intercepts and slopes of the plot [37].

The comparison of the experimental and predicted breakthrough curves at different bed depth (flow rate 4 mL/min) and flow rate (bed depth 1 cm) according to Thomas model are shown in Figs. 7 and 8, respectively. Meanwhile, a linear regression analysis was used to evaluate the Thomas model parameters and the results are presented in Table 2. It indicates that predicted and experimental value were all acceptable fits to Thomas model which the values of $\varepsilon\%$ are lower. As flow rate increased, the values of k_{Th} increased from 6.30×10^{-3} to $9.15 \times 10^{-3} \text{L}/\mu\text{mol h}$ and the values of N_0 decreased from 71.01 to 46.98 $\mu\text{mol/g}$. The N_0 increased with increasing bed depth, but the coefficient k_{Th} changed irregularly. Therefore, lower flow rate and higher bed depth was benefit to bromate removal in the Fe–Al LDH column. The well fit of the experimental data to the Thomas model

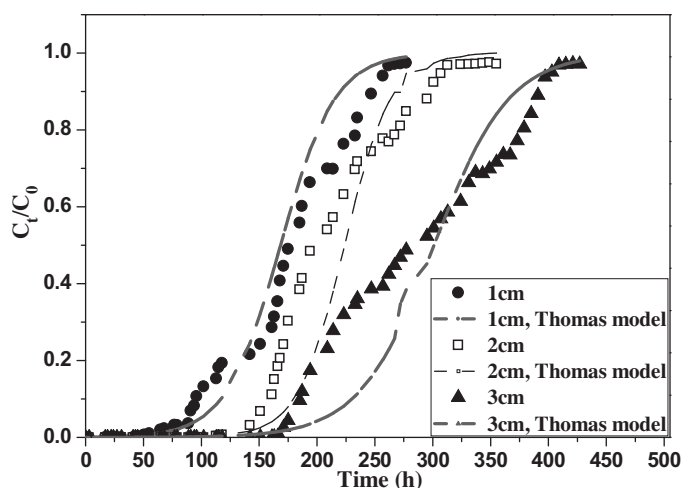


Fig. 7. Application of Thomas model to the experimental data obtained at different bed depth (initial bromate concentration $6.25 \mu\text{mol/L}$ and flow rate 4 mL/min).

illustrated that the external and internal diffusion was not the limiting step [38], and the bromate removal process in Fe–Al LDH followed to pseudo-first-order kinetics [15].

Comparison between applied models

As shown in Table 2, the values of R^2 for BDST model were slightly higher than the value of the Thomas model, but some studies suggested that BDST model cannot be validated only by analyzing the R^2 for the more significant effect to the accuracy during the linear regressive analysis [39]. The nonlinear regressive analysis can be a better option in avoiding such errors and more effective [40]. For the BDST model, the predicted results were much in agreements to the experimental at breakthrough of 1% and 10% with $\varepsilon\%$ value of 6.67% and 9.91%, respectively. However, after 10% breakthrough, the error values increased to 17.24–28.94%. These data suggested the better conformity of BDST model for bromate removal by Fe–Al LDH only lower breakthrough (below 10%). Other literature also demonstrated that the BDST model cannot be validated for the whole breakthrough stage [39]. Furthermore, it was found that values of $\varepsilon\%$ for Thomas were lower than those for BDST model. Thus, Thomas model is more suitable for describing the behavior of bromate removal by Fe–Al LDH.

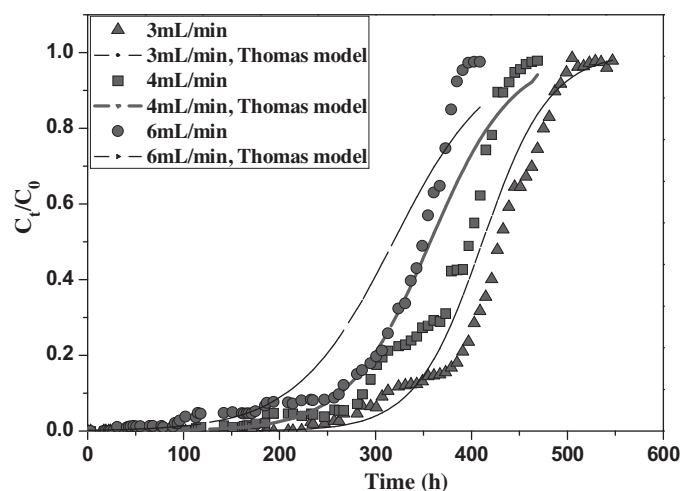


Fig. 8. Application of Thomas model to the experimental data obtained at different flow rate (initial bromate concentration $6.25 \mu\text{mol/L}$ and bed depth 1 cm).

Conclusions

Fe(II)–Al(III) layered double hydroxide (Fe–Al LDH) shows excellent adsorption-coupled reduction ability to the bromate in the solution due to the existence of Fe(II). In this study, an extensive laboratory investigation was conducted to evaluate the Fe–Al LDH fixed-bed column performance for bromate removal. The effects of bed depth, flow rate, and initial bromate concentration on breakthrough curves were investigated. The column experimental data were analyzed using BDST and Thomas models, while the BDST model can represent the initial part of the breakthrough curve at the breakthrough point (C_t/C_0) of 1 and 10%. The rate constant and dynamic removal capacity at 1% breakthrough were calculated as $0.55 \times 10^{-3} \text{ L}/\mu\text{mol h}$ and $18.99 \times 10^3 \mu\text{mol/L}$, respectively. Thomas model well described the whole breakthrough curves at the various experimental conditions. Based on the value of maximum removal capacity (N_0), lower flow rate and higher bed depth was benefit to remove bromate by Fe–Al LDH in fixed-bed column.

Acknowledgements

This research was financially supported by the project of National Natural Science Foundation of China (No. 51378188, 51278175) and Doctoral Fund of Ministry of Education of China (20130161120021) and the Fundamental Research Funds for the Central Universities.

References

- [1] U. von Gunten, *Water Res.* 37 (2003) 1469.
- [2] R. Mack, *N. C. Med. J.* 49 (1988) 243.
- [3] M. Deshimaru, T. Miyagawa, S. Sumiyoshi, Y. Nomura, *Brain* 28 (1976) 807.
- [4] H.S. Weinberg, C.A. Delcomyn, V. Unnam, *Environ. Sci. Technol.* 37 (2003) 3104.
- [5] S.W. Krasner, W.H. Glaze, H.S. Weinberg, P.A. Daniel, I.N. Najm, *J. Am. Water Works Assoc.* 85 (1993) 73.
- [6] M.L. Bao, O. Griffini, D. Santianni, K. Barbieri, D. Burrini, F. Pantani, *Water Res.* 33 (1999) 2959.
- [7] Q. Wang, S. Snyder, J. Kim, H. Choi, *Environ. Sci. Technol.* 43 (2009) 3292.
- [8] A. Bhatnagar, Y. Choi, Y. Yoon, Y. Shin, B.H. Jeon, J.W. Kang, *J. Hazard. Mater.* 170 (2009) 134.
- [9] K. Listiarini, J.T. Tor, D.D. Sun, J.O. Leckie, *J. Membr. Sci.* 365 (2010) 154.
- [10] R. Chitrakar, A. Sonoda, Y. Makita, T. Hirotsu, *Ind. Eng. Chem. Res.* 50 (2011) 9280.
- [11] S. Li, Y. Shen, M. Xiao, D. Liu, L. Fa, K. Wu, *J. Ind. Eng. Chem.* 20 (2014) 1280.
- [12] R.r. Shan, L.g. Yan, Y.m. Yang, K. Yang, S.j. Yu, H.q. Yu, B.c. Zhu, B. Du, *J. Ind. Eng. Chem.* 21 (2015) 561.
- [13] R. Chitrakar, A. Sonoda, Y. Makita, T. Hirotsu, *Sep. Purif. Technol.* 80 (2011) 652.
- [14] R. Chitrakar, Y. Makita, A. Sonoda, T. Hirotsu, *J. Colloid Interface Sci.* 354 (2011) 798.
- [15] Y. Zhong, Q. Yang, K. Luo, X. Wu, X. Li, Y. Liu, W. Tang, G. Zeng, B. Peng, *J. Hazard. Mater.* 250–251 (2013) 345.
- [16] S. Kundu, A. Gupta, *J. Colloid Interface Sci.* 290 (2005) 52.
- [17] S. Mossa Hosseini, B. Ataie-Ashtiani, M. Kholghi, *Desalination* 276 (2011) 214.
- [18] L. Monser, N. Adhoum, *Sep. Purif. Technol.* 26 (2002) 137.
- [19] P. Suksabye, P. Thiravetyan, W. Nakbanpote, *J. Hazard. Mater.* 160 (2008) 56.
- [20] E.R. Monazam, J. Spenik, L.J. Shadle, *Chem. Eng. J.* 223 (2013) 795.
- [21] X. Sun, T. Imai, M. Sekine, T. Higuchi, K. Yamamoto, A. Kanno, S. Nakazono, *J. Ind. Eng. Chem.* 20 (2014) 3623.
- [22] M.A. Acheampong, K. Pakshirajan, A.P. Annachatre, P.N.L. Lens, *J. Ind. Eng. Chem.* 19 (2013) 841.
- [23] H.P. Chao, C.C. Chang, A. Nieva, *J. Ind. Eng. Chem.* 20 (2014) 3408.
- [24] J. Paul Chen, J.T. Yoon, S. Yiacoumi, *Carbon* 41 (2003) 1635.
- [25] K. Vijayaraghavan, J. Jegan, K. Palanivelu, M. Velan, *Chem. Eng. J.* 106 (2005) 177.
- [26] D.C. Ko, J.F. Porter, G. McKay, *Chem. Eng. Sci.* 55 (2000) 5819.
- [27] E. Malkoc, Y. Nuhoglu, Y. Abali, *Chem. Eng. J.* 119 (2006) 61.
- [28] R. Chitrakar, Y. Makita, A. Sonoda, T. Hirotsu, *J. Hazard. Mater.* 185 (2011) 1435.
- [29] K.H. Goh, T.T. Lim, *J. Hazard. Mater.* 180 (2010) 401.
- [30] X. Xu, D. Li, J. Song, Y. Lin, Z. Lv, M. Wei, X. Duan, *Particology* 8 (2010) 198.
- [31] K.-H. Goh, T.-T. Lim, Z. Dong, *Water Res.* 42 (2008) 1343.
- [32] N. Chubar, *J. Colloid Interface Sci.* 357 (2011) 198.
- [33] S. Ghorai, K.K. Pant, *Chem. Eng. J.* 98 (2004) 165.
- [34] G. Bohart, E. Adams, *J. Am. Chem. Soc.* 42 (1920) 523.
- [35] A. Adak, A. Pal, *Sep. Purif. Technol.* 50 (2006) 256.
- [36] R.A. Hutchins, *Chem. Eng.* 80 (1973) 133.
- [37] G. Yan, T. Viraraghavan, *Bioresour. Technol.* 78 (2001) 243.
- [38] R. Han, Y. Wang, X. Zhao, Y. Wang, F. Xie, J. Cheng, M. Tang, *Desalination* 245 (2009) 284.
- [39] P.A. Kumar, S. Chakraborty, *J. Hazard. Mater.* 162 (2009) 1086.
- [40] R. Han, Y. Wang, W. Zou, Y. Wang, J. Shi, *J. Hazard. Mater.* 145 (2007) 331.